DECOUPLING HAMP FROM TM2 IN THE *ESCHERICHA COLI* ASPARTATE CHEMORECEPTOR

A Senior Scholars Thesis

by

RACHEL LEANN CROWDER

Submitted to the Office of Undergraduate Research
Texas A&M University
in partial fulfillment of the requirements for the designation as

UNDERGRADUATE RESEARCH SCHOLAR

April 2009

Major: Biology

DECOUPLING HAMP FROM TM2 IN THE *ESCHERICHA COLI* ASPARTATE CHEMORECEPTOR

A Senior Scholars Thesis

by

RACHEL LEANN CROWDER

Submitted to the Office of Undergraduate Research
Texas A&M University
in partial fulfillment of the requirements for the designation as

UNDERGRADUATE RESEARCH SCHOLAR

Approved by:

Research Advisor: Michael D. Manson
Associate Dean for Undergraduate Research: Robert C. Webb

April 2009

Major: Biology

ABSTRACT

Decoupling HAMP from TM2 in the *Escherichia coli* Aspartate Chemoreceptor.
(April 2009)

Rachel Leann Crowder
Department of Biology
Texas A&M University

Research Advisor: Dr. Michael D. Manson
Department of Biology

The HAMP (often found in Histidine kinases, Adenylate cyclases, Methyl-accepting chemotaxis proteins, and Phosphatases) domain is a widely conserved motif often found in transmembrane signaling proteins in many prokaryotes and lower eukaryotes. It consists of a pair of two amphipathic helices connected by a flexible linker. Recently, the solution structure of the *Archeoglobus fulgidis* Af1503 HAMP domain was isolated and resolved using NMR. The Af1503 HAMP domain forms a stable four helix bundle with parallel helices that pack into a non-canonical knob-on-knob conformation. Several models have been proposed in methyl-accepting chemotaxis proteins (MCPs) to explain how the four-helix bundle transmits the downward piston movement of transmembrane 2 (TM2) into the signaling domain, inhibiting kinase activity. It is likely the connector between TM2 and the HAMP domain is important in transducing the input signal from TM2 to HAMP. Following this rationale, increasing the flexibility of the connector should reduce the intensity of the output signal. To test the effect of increasing the flexibility of the TM2/HAMP linker, residues methionine 215 through threonine 218 of

the *Escherichia coli* aspartate chemoreceptor Tar were replaced with four glycine residues. Glycine residues were then deleted (-1G through -4G) and added (+1G through +5G). Aspartate sensitivity, rotational bias, mean reversal frequency, and *in vivo* methylation levels were measured. These experiments suggest that increasing the flexibility between TM2 and HAMP reduces the strength of signal transmission from TM2 to HAMP, and places the receptor in an inactive form that mimics the attractant-bound state.

DEDICATION

This manuscript is dedicated to my mother and father for their endless support and constant encouragement to pursue my dreams and to never stop learning. Thanks, Mom and Dad.

ACKNOWLEDGMENTS

Many people have played an integral part in my successes. I would like to thank all of those who have helped me become a researcher. I am sincerely grateful for the love and support my family has given. Without their encouragement and hard work, I would not be the scholar I am today. I would especially like to thank my brother for providing me a role model to follow while growing up. His brilliance inspired me to strive to attain my full intellectual potential.

I am grateful for my research advisor, Dr. Michael Manson. I could not ask for a better advisor. He has given me countless opportunities to speak with and learn from some of the finest minds, and he has played a monumental role in helping me harness my creativity and ability to critically think.

I would also like to acknowledge the National Science Foundation LSAMP program and the Bartoszek Fund for providing the funds from which the research was performed.

Finally, I would like to thank the members of the Manson Lab for providing a friendly, supportive atmosphere. I especially want to recognize Drs. Roger Draheim and Run-zhi Lai for teaching me new techniques and helping troubleshoot problems that arose. Above all, I wish to thank my fellow lab-mate, mentor, and best friend Dr. Gus Wright, who spent countless hours helping me design and run experiments. I appreciate his

willingness to collaborate with me and share his research with me. It was through his efforts that I now have a deeper understanding of this world. I will be forever grateful for his mentorship and continued support.

NOMENCLATURE

AS1	amphipathic helix 1
AS2	amphipathic helix 2
CCW	counterclockwise
CD	cytoplasmic domain
Che	chemotaxis protein
CW	clockwise
HAMP	histidine kinase, adenylate cyclase, methyl-accepting chemotaxis protein, phosphatase
HPK	histidine protein kinase
MCP	methyl-accepting chemotaxis protein
MRF	mean reversal frequency
NMR	nuclear magnetic resonance
SDS	sodium dodecyl sulfate
TM2	transmembrane 2

TABLE OF CONTENTS

Page

ABSTRACT iii

DEDICATION v

ACKNOWLEDGMENTS vi

NOMENCLATURE viii

TABLE OF CONTENTS ix

LIST OF FIGURES xi

CHAPTER

I INTRODUCTION 1

E. coli motility and chemotaxis 1
Allosteric signaling regulates cellular behavior through the induction of a phosphorelay system 3
Chemoreceptors transmit environmental stimuli 5
Solving the structure of HAMP 10
Understanding HAMP's role in signal conversion 10

II MATERIALS AND METHODS 12

Bacterial strains and plasmids 12
Measuring protein expression 12
Measuring motility and chemotaxis towards attractant 13
Observing tethered cells 13

III RESULTS 15

Decoupling HAMP from TM2 15
Receptor sensitivity towards aspartate 17
Observing flagellar motor rotation 17

IV DISCUSSION AND CONCLUSIONS 24

REFERENCES 29

Page

CONTACT INFORMATION 34

LIST OF FIGURES

FIGURE Page

1 Chemotaxis of *E. coli* in a chemoeffector gradient 2

2 Flagellar rotation controlled by phosphorelay 7

3 The chemoreceptor homodimer 9

4 Introduction of Gly residues create a flexible tether 16

5 Glycine mutant aspartate swarm rates 18

6 Glycine mutant mean reversal frequencies 20

7 Flagellar rotational bias as a result of methylation compensation 21

8 Flagellar rotational bias without adaptation 23

9 Schematic illustration of the chemoreceptors influence on ChA kinase activity in the absence of adaptation machinery ($CheR^{-}B^{-}$) 28

CHAPTER I

INTRODUCTION

Escherichia coli is a rod-shaped, gram-negative bacterium. It is approximately 2μm long and 0.5-1.0μm in diameter. An *E. coli* cell is too small to affect its environment appreciably; thus, a cell must continuously monitor its surroundings and take appropriate measures to ensure survival. *E. coli*, along with many other prokaryotes and eukaryotes, uses chemotaxis to move up or down gradients of environmental stimuli (*1*), such as pH (*2*), redox potential (*3, 4*), amino acids (*5*), sugars(*6*), metal ions, and small peptides(*7*).

E. coli motility and chemotaxis

E. coli have five to seven petrichous flagella located randomly around the cell (*8*). A bi-directional proton-driven motor at the cytoplasmic base of each flagellum allow rotation of each flagellum. Motors turn either clockwise (CW) or counterclockwise (CCW) (*9*). During counterclockwise rotation, the flagellar filaments coalesce to form a bundle that propels the cell in a smooth swim, called a run (*10*). Clockwise rotation dissociates this bundle, thereby allowing the cell to reorient itself in three-dimensional space—an event known as a tumble (*11*) (Figure 1, Part A). The rate of reorientation is determined by the number of flagella involved in a clockwise motion.

This thesis follows the style of *Biochemistry*.

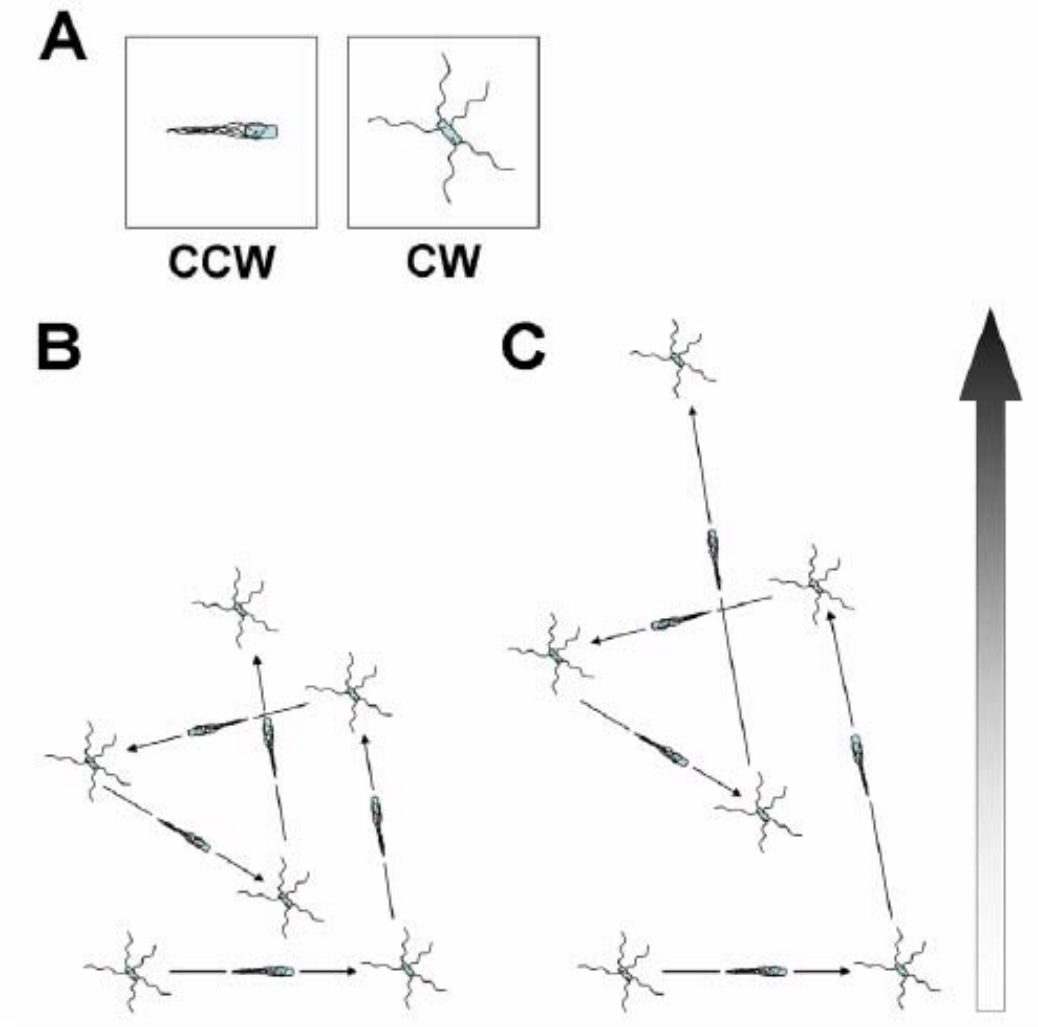

Figure 1: Chemotaxis of *E. coli* in a chemoeffector gradient. (A) Counterclockwise (CCW) rotation causes the flagellar filaments to coalesce into a bundle that propels the cell in a run. Clockwise rotation (CW) dissociates the bundle, causing the cell to reorient itself in three-dimensions—a tumble. (B) In an environment lacking attractant or repellent, cells carry out a random walk, alternating between runs and tumbles. (C) In a gradient of chemoeffector, runs in the favorable direction are extended, thus biasing the random walk and allowing for overall migration toward higher concentrations of attractant (shaded region) or lower concentrations of repellent.

In an environment lacking a detectable chemical gradient, the flagellar motor alternates between CCW and CW rotation, causing the cell to execute a three-dimensional random walk (Figure 1, Part B). The cell continuously assesses its surroundings in order to compare its current chemical environment to the one it occupied in the recent past (~3 seconds) (*12, 13*). The cell uses this information to continue swimming in its present direction or to randomly reorient itself to sample a new direction (*12, 14, 15*). *E. coli* initiates a biased three-dimensional walk when unidirectional smooth-swimming runs become longer because tumbling events become less frequent (Figure 1, Part C).

Allosteric signaling regulates cellular behavior through the induction of a phosphorelay system

These physiological responses are the result of the phosphorelay signaling cascade triggered by external stimuli sensed by the chemoreceptors. In *E. coli* this pathway is controlled by four transmembrane chemoreceptors and a set of cytosolic chemotaxis (Che) proteins. The internal phosphorelay system begins with the histidine protein kinase (HPK), CheA, which undergoes autophosphorylation that is stimulated by contact of the CheA dimer with the basal tip of the chemoreceptor cytoplasmic domain (*16-18*). This coupling also requires the CheW protein (*19*). In the absence of ligand, CheA is allosterically induced to its "on" state, and autophosphorylates at His48 in the N-terminal P1 domain. The response regulator, CheY, then binds to the P2 domain of CheA, and the phosphoryl group is transferred to Asp57 of CheY to produce phospho-CheY (CheY-P). CheY-P has a much lower affinity for CheA than CheY and quickly

dissociates from the kinase. CheY-P diffuses through the cytosol to the flagellar motor, where it interacts with FliM (*20-22*), the protein responsible for motor switching. As the concentration of intracellular CheY-P increases, more CheY-P associates with FliM throughout the cell to induce a reversal of the flagellar motor to CW rotation (*23, 24*). This reversal causes a tumbling event. As the concentration of intracellular CheY-P decreases, the flagellar motor resumes a CCW rotation. Although CheY-P spontaneously dephosphorylates of CheY-P, its dephosphorylation by the phosphatase, CheZ, ensures that the steady-state ratio of CheY and CheY-P is maintained in the cell that results in frequent switching between CW and CCW flagellar rotation (*22, 25-27*).

When an attractant binds, the ability of the receptor to stimulate CheA is inhibited. This inhibition is transient because the ligand-induced changes are counterbalanced by methylation of specific amino acid residues within the adaptation region of the receptor. The methyltransferase CheR adds methyl groups to Glu295, 302, 309, and 491 (*28*), leading to four methyl-glutamyl residues per receptor monomer in the fully methylated state. Methyl groups are removed by the methylesterase CheB, which is activated by phosphorylation by CheA (*29, 30*). Increased methylation increases CheA stimulation, and decreased methylation decreases CheA stimulation (a schematic illustration of the circuit is shown in Figure 2).

Chemotaxis is the result of the interplay between the phosphorelay and the adaptation machinery. Without either system, cells could bind to chemoeffectors but would be

unable to respond by moving up or down a particular chemical gradient. This is because the methylation of the adaptation region serves as a "memory" for the cell. Due to short lag between the initial ligand-induced signal and the compensating methylation, the cell is able to store "information," in the form of methylated residues, about the previous surrounding environment. Because of this, the cell has the ability to compare two environments and move toward the more favorable direction.

Chemoreceptors transmit environmental stimuli

E. coli has five different transmembrane chemoreceptors that sense changes in chemical concentrations outside the cell. These include the serine chemoreceptor, Tsr; the aspartate/maltose chemoreceptor, Tar; the ribose/galactose-glucose chemoreceptor, Trg; and the dipeptide/pyrimidine chemoreceptor, Tap (*7, 31-34*). There is also a receptor involved in detecting redox potential, Aer (*3*). All of these chemoreceptors are methyl-accepting chemotaxis proteins (MCP's), except Aer, which lacks the adaptation region to which methyl groups would normally be attached (*35*). Each chemoreceptor regulates the histidine kinase, CheA. Since CheA is inhibited by attractant binding to the periplasmic region of the chemoreceptor, the attractant is a negative allosteric effector of CheA.

Tsr and Tar, the two most abundant chemoreceptors in *E. coli*, correspondingly elicit the strongest chemotactic responses. These proteins function as organized oligomers, forming trimers of dimers under normal cellular conditions (*17, 36-39*). The homodimer, however, appears to be the smallest functional unit of all MCP's, with each peptide chain running parallel to the other. Within each homodimer, five distinct domains exist (*40*)—the periplasmic domain, the transmembrane region, the HAMP domain, the adaptation region, and the signaling domain (the latter two compose the cytoplasmic domain) (Figure 3). The periplasmic domain resides in the periplamic space. It consists of a four-helix bundle that creates a pocket to which ligand binds (*41-43*). The transmembrane region is composed of two hydrophobic helices—transmembrane 1 (TM1) and transmembrane 2 (TM2)—that connect the periplasmic domain to the cytoplasm. TM2 is thought to propagate the conformational change created by the binding of ligand to the periplasmic region to the cytoplasmic domain

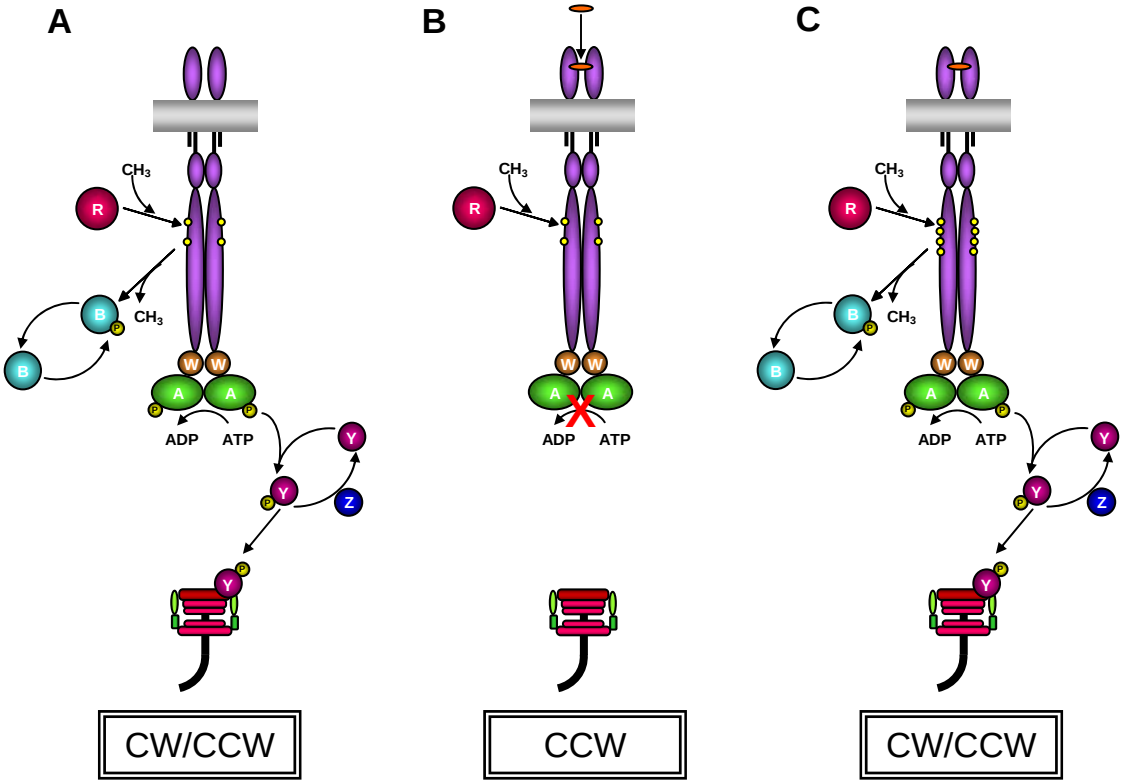

Figure 2: Flagellar rotation controlled by phosphorelay. (A) In the absence of ligand, CheA maintains production of phospho-CheY, resulting in a three-dimensional random walk. (B) Upon binding of attractant, CheA stimulation stops. This reduces the level of inner cellular phospho-CheY, thereby reducing the probability of a tumbling event and increasing the likelihood of a run. (C) Methylation of the adaptation region reactivates CheA, restoring the cell to a pre-stimulus state.

through a downward piston-like motion through the membrane (*44-46*). This signal is received by the HAMP (Histidine kinase, Adenylate cyclase, Methyl-accepting chemotaxis protein, Phosphatase) domain, which lies adjacent to the cell membrane. HAMP is composed of two amphipathic helices, AS1 and AS2, which are connected by a flexible connector, creating a parallel four-helix bundle in its dimeric state (*47, 48*). Input signals pass through this region and are converted into conformational changes that can be communicated to the cytoplasmic domain. The cytoplasmic domain is an extended four-helix bundle (composed of CD1, CD2, CD1', and CD2') that encompasses the adaptation region and the signaling domain (*17*). Signals propagated through HAMP pass through the adaptation region to the signaling domain, where they induce a change in the helical packing of CD1, CD2, CD1', and CD2'. Tighter packing of these helices triggers the autophosphorylation of CheA, whereas looser packing inhibits CheA (*49-51*).

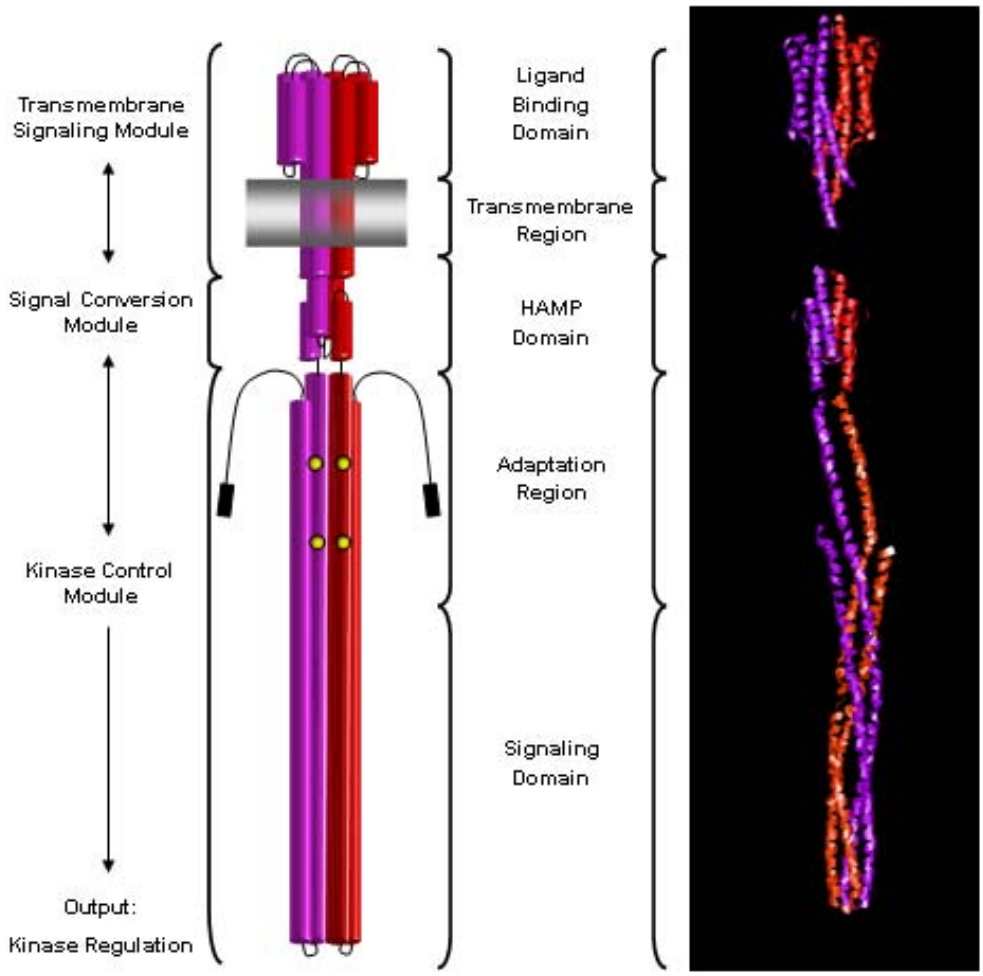

Figure 3: The chemoreceptor homodimer. A cartoon (left) and a ribbon structure (right) illustrate the structure of the Tar homodimer. Modules (transmembrane signaling, signal conversion, and kinase control) depicted on the far left indicate regulatory regions of the receptor. The functional domains (ligand binding, transmembrane, HAMP, adaptation, and signaling) of the receptor are indicated in the center

Solving the structure of HAMP

Although chemoreceptors have been well characterized and have provided much insight into the mechanism of receptor-mediated transmembrane signaling, one region of these proteins have remained elusive to the fine-toothed comb of science. Due to their dynamic nature, it is difficult to isolate the transmembrane region and HAMP domain of MCP's for study. For this reason, much still remains unknown about how HAMP and TM2 transmit signals to the cytoplasmic domain. Recently, the solution structure of the *Archeoglobus fulgidis* Af1503 HAMP domain was resolved using NMR (*52*). The Af1503 HAMP domain forms a stable, parallel four-helix bundle composed of two amphipathic helices connected by a flexible linker which packs into a non-canonical knob-on-knob conformation. It remains unknown whether this protein assumes a similar structure in the *E. coli* chemoreceptors. However, recent disulfide-crosslinking studies using the Tar, Tsr, and Aer HAMP domains can be modeled on the Af1503 structure (*53*).

Understanding HAMP's role in signal conversion

The Af1503 structure constitutes only one state (presumably the most stable) of the dynamic HAMP domain. Signal transduction may very well involve movement between two or more conformations, making it difficult to understand the molecular mechanisms that govern HAMP dynamics and its role on signal output. To further understanding of the relationship between possible HAMP conformations and receptor function, we designed an experiment to test the effect of modifying the coupling between TM2 and

HAMP in the *E. coli* aspartate chemoreceptor, Tar. Flexibility of the TM2-HAMP linker was increased by replacing the native residues in this region with glycine residues in an. As a result, we observed the nature of signal transduced by TM2 and the role HAMP plays in transmitting this signal to the cytosol. The result was an apparent uncoupling of TM2 and HAMP, suggesting that the structure of this connector is an important aspect of transmembrane signaling.

CHAPTER II

MATERIALS AND METHODS

Bacterial strains and plasmids

Strains RP3098 (Δ(*flhD-flhB)4*) and VB13 (*thr*$^+$ *eda*$^+$ Δ*tsr7201 trg::*Tn*10* Δ*tar-tap5201*) are derived from the *E. coli* K-12 strain RP437. Strain HCB436 is VB13 Δ*cheRcheB*. Plasmid pMK113CV5, a derivative of pBR322 with an additional C-terminal seven-residue linker (GGSSAAG) and V5 epitope attached to the 3' end of *tar*, was utilized to express the mutated *tar* gene at physiological concentrations. Plasmid pBAD18 was used to over-express *tar*. Mutations were introduced into the *tar* gene via standard site-directed mutagenesis (Stratagene).

Measuring protein expression

Cells were grown in 15 mL of Luria Broth containing 100 μg/mL ampicillin overnight at 30ºC. Cultures were back diluted 1:100 in fresh medium to obtain an optical density at 600 nm (OD_{600}) of ~0.1. Cultures were shaken at 30ºC for another 5.5 hours until an OD_{600} of ~0.6 was reached. Cells were resuspended in 2X SDS loading buffer and boiled for 5 minutes. The cells were subjected to 3 freeze/boil cycles, each lasting 10 minutes in order to degrade protein. Ten μL of the protein samples were loaded into a 7.5% SDS-PAGE gel. Current was applied to the gel in order to separate bands of protein based on molecular weight. Once electrophoresis was complete, protein from the gels was transferred to nitrocellulose paper. A Western blot was performed by

adding anti-V5 eptiope goat-anti-mouse antibody (Invitrogen) to the nitrocellulose paper. Visualization of protein was achieved using goat-anti-mouse antibody conjugated to an alkaline phosphotase (Bio-Rad).

Measuring motility and chemotaxis towards attractant

Swarm assays were conducted to measure motility and chemotaxis towards attractant. Semi-solid motility media agar plates were made with the addition of 3.25 g/L BD Bacto agar, Che salts (10mM potassium phosphate (pH 7.0), 1mM $(NH_4)_2SO_4$, 1mM Mg SO_4, 1mM glycerol), 1mM $MgCl_2$, 90 mM NaCl, 0.1mM attractant (aspartate or maltose), 200 μM IPTG, 0.2% THM, 0.1% B1 vitamin, and 100 μg/mL ampicillin. Plates were inoculated with isolated colonies and incubated at 30ºC. First measurements (ring diameter in centimeters) were taken after 8 hours at 30ºC. Subsequent measurements were taken every 4 hours until colonies had swarmed for 24 hours. The rate of ring expansion is expressed in mm/hour and normalized against wild-type values.

Observing tethered cells

Cultures were grown as described previously, however with a few modifications. Cells were grown in tryptone broth with the addition of 50 μg/mL ampicillin. After cultures reached an OD_{600} of ~0.6, cells were harvested by centrifugation and resuspended in tethering buffer, containing 10 mM potassium phosphate, pH 7.0, 0.1 M NaCl, 0.01 mM EDTA, 0.02 mM L-methionine, and 20 mM sodium lactate. The addition of 20 μg/mL chloramphenicol prevented the regrowth of flagella after shearing. Cells were sheared in

the 50 mL cup Waring blender 8 times for 7 sec., with 20 sec. cooling intervals. Cells were collected by centrifugation, washed 3 times and resuspended in tethering buffer with chloramphenicol. Twenty μL of a 200-fold dilution of anti-flagellar filament antibody was added to 20 μL of these cells. After allowing 12 mm glass cover slips to soak in nitric acid for 1 hour and thorough rinsing with deionized water, Apiezon-L grease was added to the edge of these cover slips and 40 μL of the cell/antibody master mix was added to the center of the cover slip. A humidity chamber was created to store cells by placing a ring of wet filter paper around a piece of dry filter paper in a Petri dish. Cover slips were placed facing upward into the humidity chamber for 30 minutes at 30ºC. After incubation, cover slips were placed into a flow chamber and non-tethered cells were washed from the solution. Cells were observed under phase contrast at 1000x magnification using an oil immersion 100x objective and 10x eyepiece on an Olympus BH-2 microscope. One hundred rotating cells were observed for 30 sec. each to determine flagellar rotational bias and flagellar switching frequency.

CHAPTER III

RESULTS

A central question in receptor biology is the mechanism by which a signal is sensed at the external tip of the receptor and is then transmitted to the cytoplasmic tip of the receptor to effect receptor activity. In this study we have attempted to understand the process in the *E. coli* chemoreceptor Tar. More specifically, we have focused on the region that connects TM2 to the signaling region. This region, known as HAMP, plays a large role in signal conversion, and mutations targeting this region drastically affect activity levels of the receptor-coupled CheA kinase.

Decoupling HAMP from TM2

This study was designed to observe the effect of decoupling HAMP from TM2 in the *E. coli* Tar chemoreceptor. To perform this task, a series of site-directed point mutations were made in the TM2-HAMP connector region. The residues Met-215 through Thr-218 were replaced with four Gly residues (4G). We hypothesized that this mutation would essentially decouple HAMP from TM2, resulting in the inability of HAMP to transmit input signals from TM2. Additional mutations were made by adding Gly residues (+1G through +5G) and deleting Gly residues one at a time (-1G through -4G) (Figure 4).

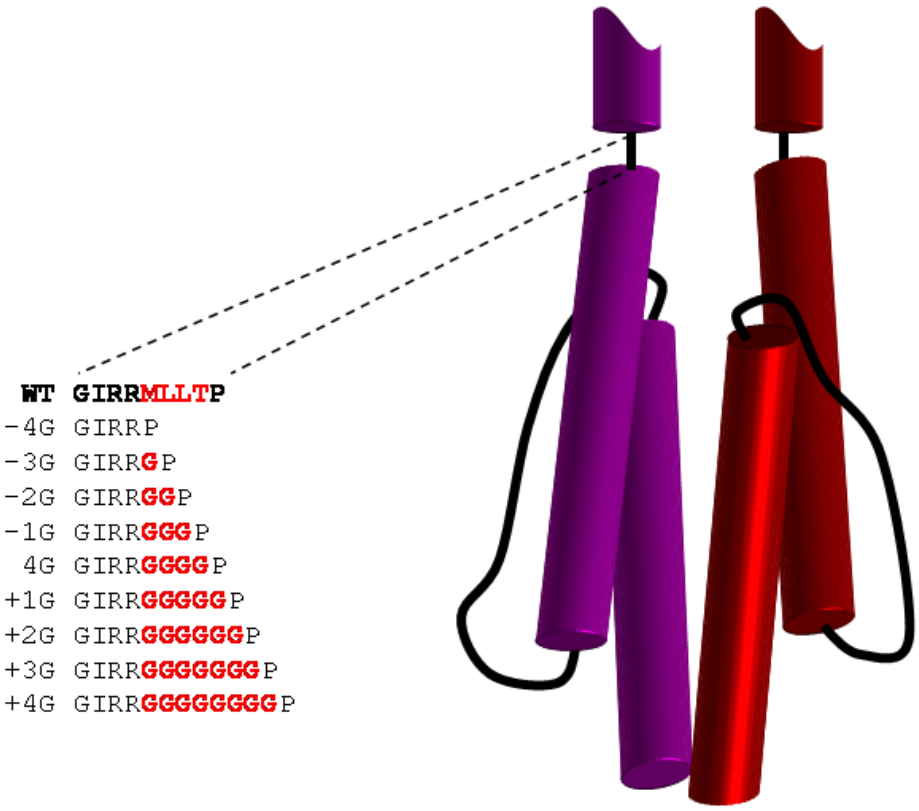

Figure 4: Introduction of Gly residues create a flexible tether. A cartoon of the HAMP domain four-helix bundle is depicted. The native TM2-HAMP linker consists of Met-215, Leu-216, Leu-217, and Thr-218. In order to introduce flexibility to region, this sequence was replace with four Gly residues (4G). Additional mutations were made by adding Gly residues (+1G through +5G) and deleting Gly residues one at a time (-1G through -4G).

Receptor sensitivity towards aspartate

A swarm plate assay provided an initial analysis of receptor function by determining whether the mutated Tar receptors were able to sense the chemoattractant aspartate. pMK113 plasmids containing the mutated *tar* genes were introduced into competent VB13 cells. Isolated colonies were stabbed into soft agar containing minimal media supplemented with aspartate. Colonies were allowed to swarm for 24 hours, at which time swarm ring diameters were measured and normalized to wild-type measurements (Figure 5). The 4G mutant had ~80% of the wild type swarm diameter. However, chemotactic ability toward aspartate drastically decreased in a stepwise manner as Gly residues were subtracted or added. The most extreme mutations, such as -3G, -4G, and +5G, exhibited a complete loss of receptor function (Figure 5).

Observing flagellar motor rotation

In order to observe the effect of the Gly-substituted TM2-HAMP tether on flagellar motor rotation, mutant pMK113CV5 plasmids were transformed into VB13. Cells were tethered to a glass slide via a single flagellum and rotational switching frequencies and rotational biases were observed for cells of each mutant in the absence of ligand in order to estimate the basal level of kinase activity induced by the Tar receptor.

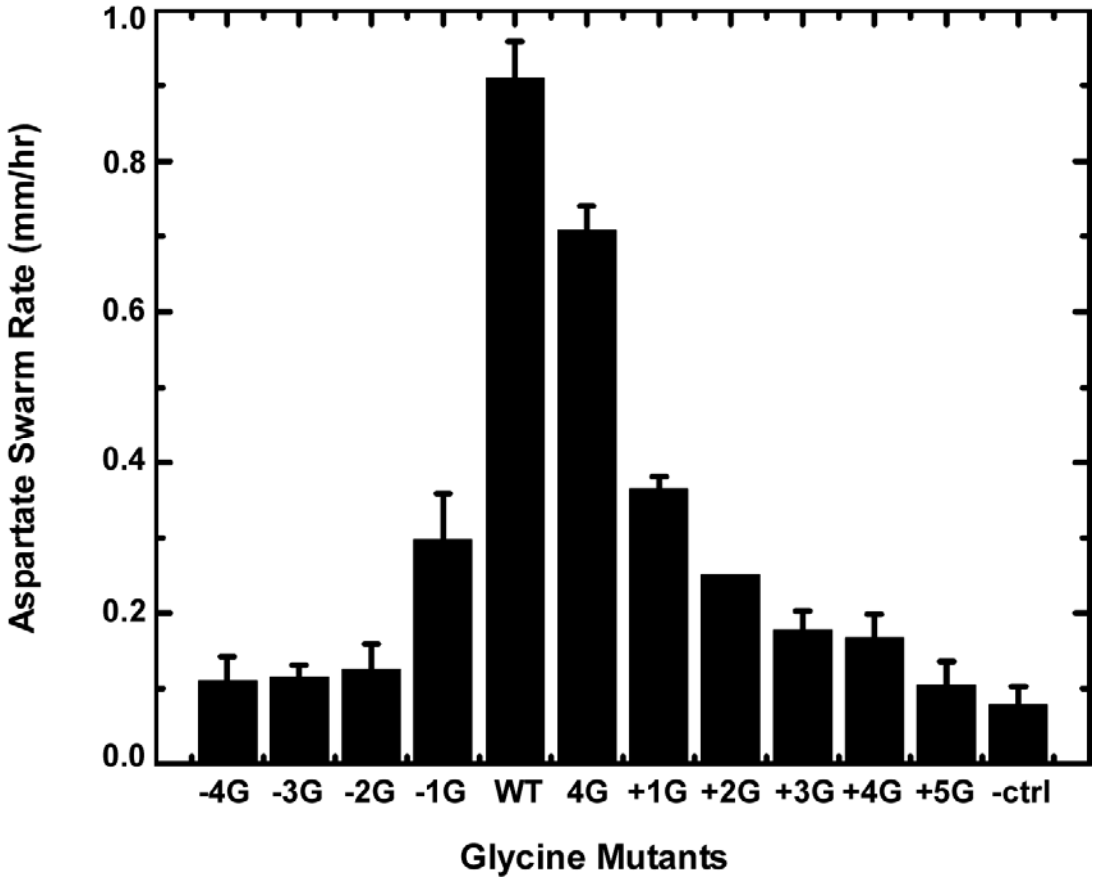

Figure 5: Glycine mutant aspartate swarm rates. Mutant receptors were expressed in pMK113CV in the VB13 strain. After 24 hours, swarm ring diameters were measured in millimeters. Rate of ring expansion is expressed as mm/hr and normalized against wild-type values.

Mean reversal frequency of cheR$^+$B$^+$ *strain*

In the CheR$^+$B$^+$ strain, wild type Tar supports a mean reversal frequency (MRF) of 0.672 reversals/sec. Substitution of the MLLT sequence with four (4G) or five Gly residue (+1G) results in comparable MRFs of 0.577 and 0.518 reversals/sec, respectively. However, the MRF drastically decreased as more Gly residues were added (+2G through +5G) or subtracted (-1G and -2G). The data is depicted in Figure 6.

Rotational bias of cheR$^+$B$^+$ *strain*

In addition to mean reversal frequencies, rotational bias was determined. Cells were separated into five groups based on the ratio of CW to CCW rotation. These groups were CCW locked, CCW biased, CCW/CW, CW biased, and CW locked. These categories correlate with CCW to CW rotation ratios of an average of 100:0, 80:20, 60:40, 20:80, and 0:100, respectively. Out of 99 WT cells, 63 exhibited an equal distribution of CCW to CW rotation, 33 cells were CCW biased, and 3 were CCW locked. The 4G mutant had very similar rotational characteristics. However, as additional Gly residues were added or subtracted, cell rotation became increasingly CCW biased and eventually became CCW locked in the -3G, -4G, and +5G mutants (Figure 7).

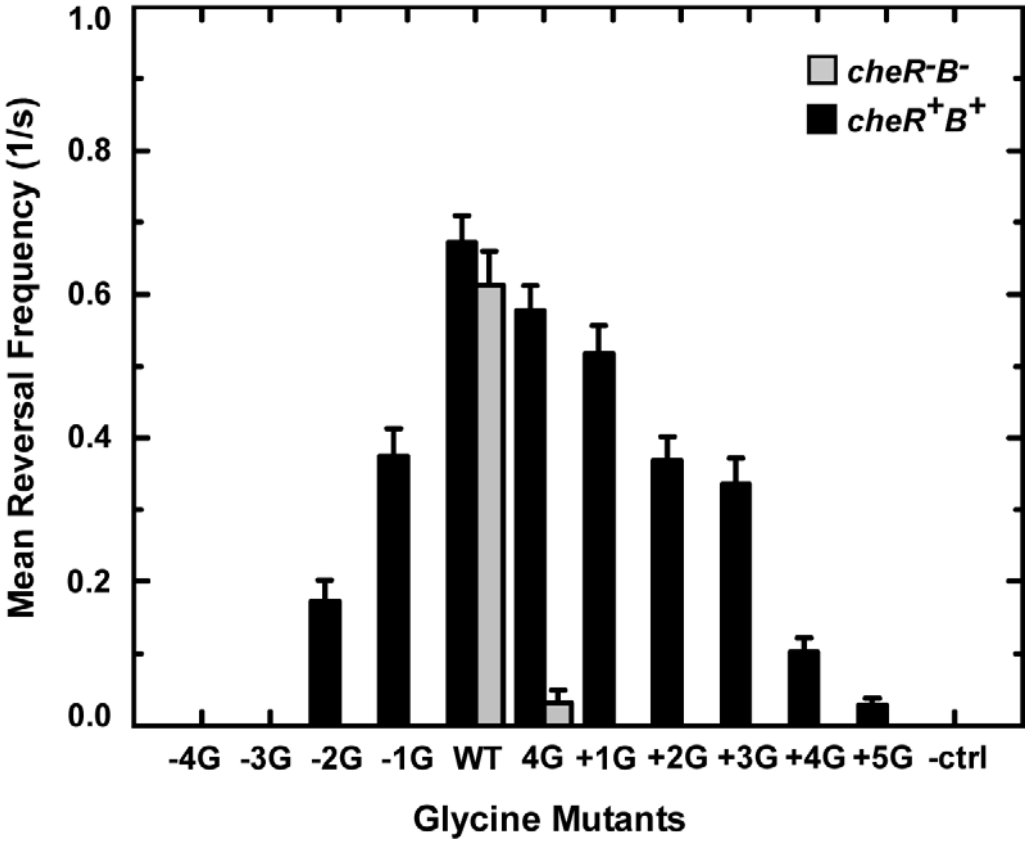

Figure 6: Glycine mutant mean reversal frequencies. Reversal frequencies of the flagellar motor were recorded for each mutant. Mean frequencies are expressed as reversal/sec, with a reversal defined a single change in direction (CW or CCW) of the flagellar motor. Cells with adaptation machinery ($cheR^+B^+$) are represented as black columns; while *ΔcheRB* cells are represented as gray columns.

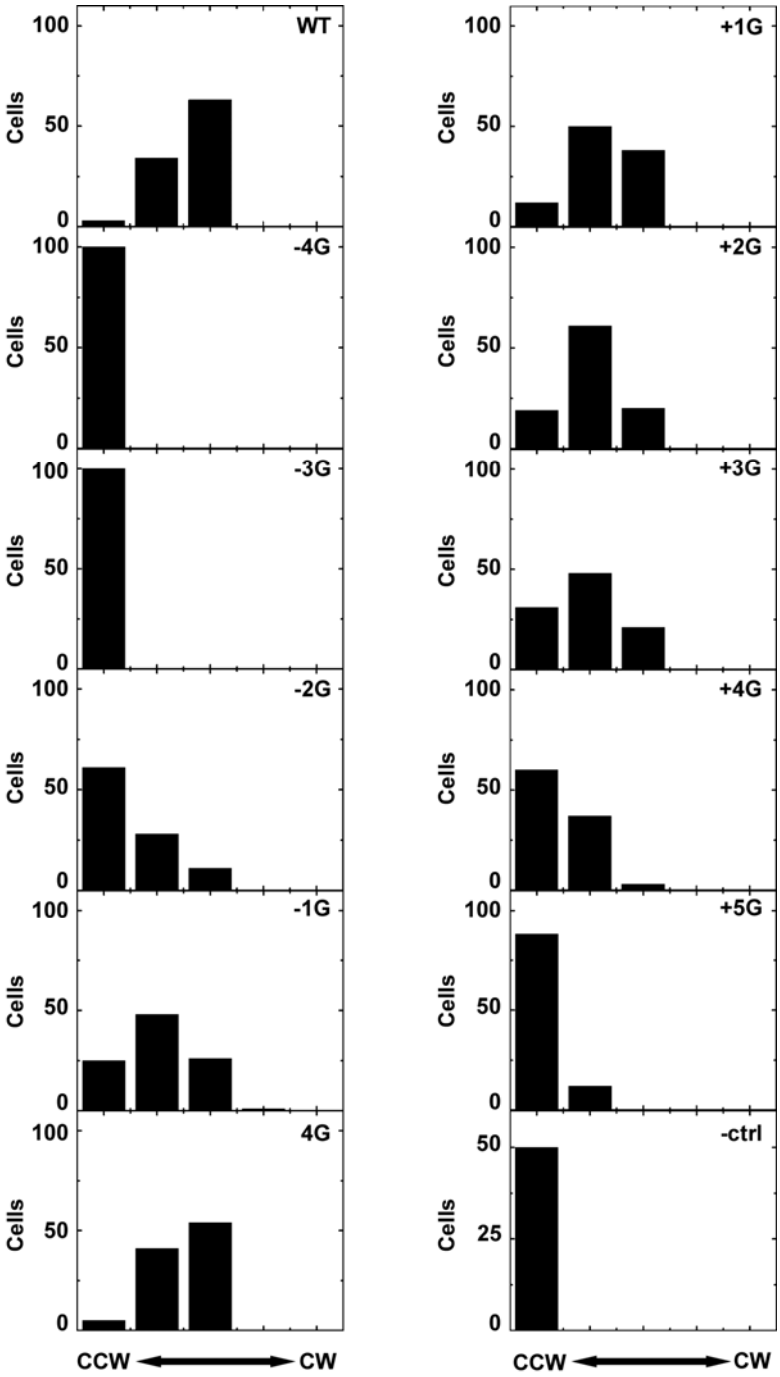

Figure 7: Flagellar rotational bias as a result of methylation compensation. The flagellar motor rotational bias during a 30 sec interval was recorded in cells expressing *cheRB*. One hundred cells per mutant were classified into five categories based on rotational bias: CCW locked, CCW biased, CCW/CW, CW biased, and CW locked (depicted graphically from left to right). Extreme Gly additions or deletions resulted in a CCW locked phenotype.

Flagellar motor characterization of the ΔcheRB *strain*

Reversal frequencies and rotational biases were observed in HCB436, a strain that lacks CheR and CheB, to understand the effects of removing the adaptation machinery. The only cells that reversed at all were those expressing the 4G mutation. These cells showed a MRF of 0.032 reversals/sec (Figure 6), with only 3 cells out of 100 experiencing reversals. Although not completely CCW locked like all of the other Gly mutants, 4G was overwhelmingly CCW biased (Figure 8).

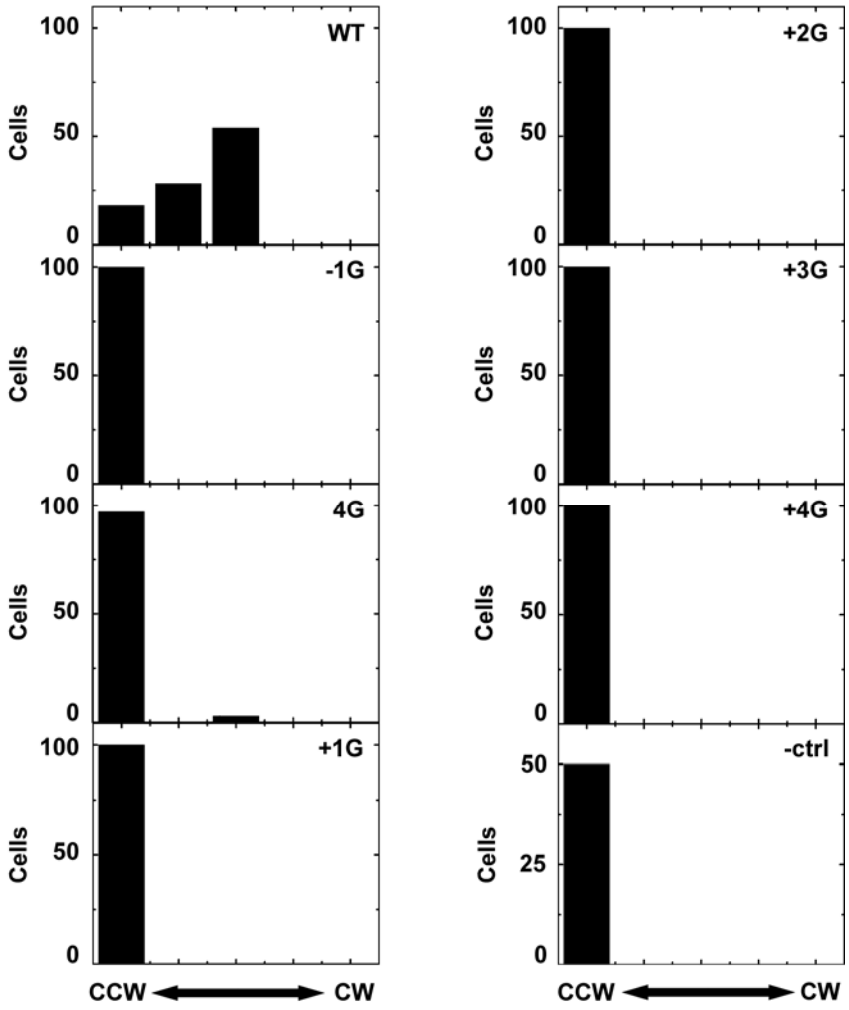

Figure 8: Flagellar rotational bias without adaptation. The flagellar motor rotational bias during a 30 sec interval was recorded in cells lacking the *cheR* and *cheB* genes. One hundred cells per mutant were classified into five categories based on rotational bias: CCW locked, CCW biased, CCW/CW, CW biased, and CW locked (depicted graphically from left to right). All mutants, except 4G, exhibited a completely CCW locked phenotype.

CHAPTER IV

DISCUSSION AND CONCLUSIONS

E. coli chemotaxis is a system that serves as a model for other two-component signaling pathways, and many of its properties are conserved in other prokaryotic and eukaryotic organisms. Recently, the focus of study has shifted to the mechanisms employed to transfer stimuli from the extracellular environment to the cell interior. This effort faces difficulties, since the cell membrane interferes with direct observation of the transmembrane region. Because of this complication, ligand binding and kinase activation have been described in detail, but the means by which the signal is transferred for the external to the internal domains remains elusive. This study has attempted to address the issue of signal propagation through the region that connects the signal input and signal output domains. We have utilized the *E. coli* aspartate chemoreceptor, Tar, to focus on the region of the receptor immediately C-terminal of, and adjacent to, TM2 and the cytosolic membrane, called the HAMP domain. We hypothesized that by replacing the native MLLT sequence of the TM2-HAMP linker with a flexible Gly-residue linker, HAMP would be decoupled from TM2, resulting in a receptor that is incapable of transducing signals initiated by ligand binding to the cytoplasmic domain.

As expected, all mutations in the TM2-HAMP linker resulted in a CCW-locked (locked off) phenotype in cells lacking adaptation machinery (HCB436 ΔcheR$^-$B$^-$). A CCW-locked phenotype suggests that the concentration of intracellular CheY-P is decreased.

This can be explained by decreased CheA kinase activity. According to these data, the receptor is locked "off" even when attractant is not present. This suggests that inserting a flexible linker (in this case, a string of Gly residues) between TM2 and HAMP alters the basal signal normally seen in a fully intact receptor.

Previous studies show that CheA is activated by the cytoplasmic domain of the receptor in the presence of CheW (*18*). However, if HAMP is added to the cytoplasmic domain, CheA activity is substantially decreased (J.S. Parkinson, personal communication). These data, and the results of this experiment, indicate that HAMP acts as an inhibitor of the kinase-activating function of the cytoplasmic domain. Kinase activity is restored when the periplasmic and transmembrane regions are present, indicating that HAMP inhibition of the cytoplasmic domain is overcome. It seems logical to conclude that the role of the periplasmic and transmembrane regions is to inhibit HAMP, therefore counteracting its inhibition of kinase-activating activity. The addition of attractant may inhibit the HAMP-override imposed by the periplasmic/transmembrane region, in which case HAMP would again inhibit stimulation of CheA, causing the flagellar motor to rotate CCW (Figure 9).

The rotational bias and reversal frequencies of the mutants are "recovered" (are closer to wild-type levels) in the presence of the adaptation system ($CheR^{+}B^{+}$). Preliminary results indicate that mutant receptors are overmethylated, suggesting that they are a good substrates for CheR but poor substrates for CheB.

Methylation of Glu residues in the adaptation region neutralizes their negative charge, decreasing the repulsion by Glu residues in the adaptation region of the other subunit in the homodimer. A tighter packing of the CD1, CD2, CD1', and CD2' helices should result. This mechanism would explain the rescue of the CCW-locked phenotype by an overmethylated receptor. Flexibility introduced into the TM2-HAMP linker may stabilize the four-helix bundle of HAMP in its inhibitory conformation, resulting in the destabilization of the four-helix bundle of the cytoplasmic domain through loosening of the helical packing. Methylation may then compensate by causing the helices to pack more tightly. Tighter packing may transfer further upstream the receptor where it may be interpreted as stabilization in HAMP. Therefore, the key to optimal chemotaxis is the maintenance of HAMP in a state of intermediate stability. Any deviation from this critical point may bias the receptor enough to shift its fine tuning away from equilibrium. Methylation by the adaptation system may provide a means to keep the receptor from deviating too far from equilibrium.

Although methylation rescued receptor function of the -1G, 4G, and +1G mutants, the more extreme mutants, such as the -3G, -4G, and +5G, did not regain kinase activity in the presence of CheR and CheB. These receptors undergo equal levels of methylation as the 4G mutant, indicating that they experience a similar level of destabilization of the four-helix bundle in the cytoplasmic domain, yet have drastically decreased chemotactic ability. If kinase activity were solely dependent upon stability in the TM2-HAMP linker

affecting the cytoplasmic domain, similar receptor sensitivity toward ligand would be expected, regardless of tether length. However, according to these results, kinase activity is dependent upon an optimal tether length. Upon shortening and lengthening the TM2-HAMP linker, methylation is incapable of restoring CheA kinase activity. This difference suggests that the signal created by the binding of attractant is not being completely transferred to HAMP. Input signals are thus dampened or completely lost by a longer or shorter tether, suggesting that signal propagation from TM2 to HAMP is determined by the length of the TM2-HAMP linker.

From these data, it is evident that increasing the flexibility and changing the length of the TM2-HAMP linker decouples the TM2 input signal from the cytoplasmic domain's output signal, because CheA kinase is inhibited by the introduction of multiple Gly residues. If the effect is not too large, however, receptors are capable of being rescued by increased methylation.

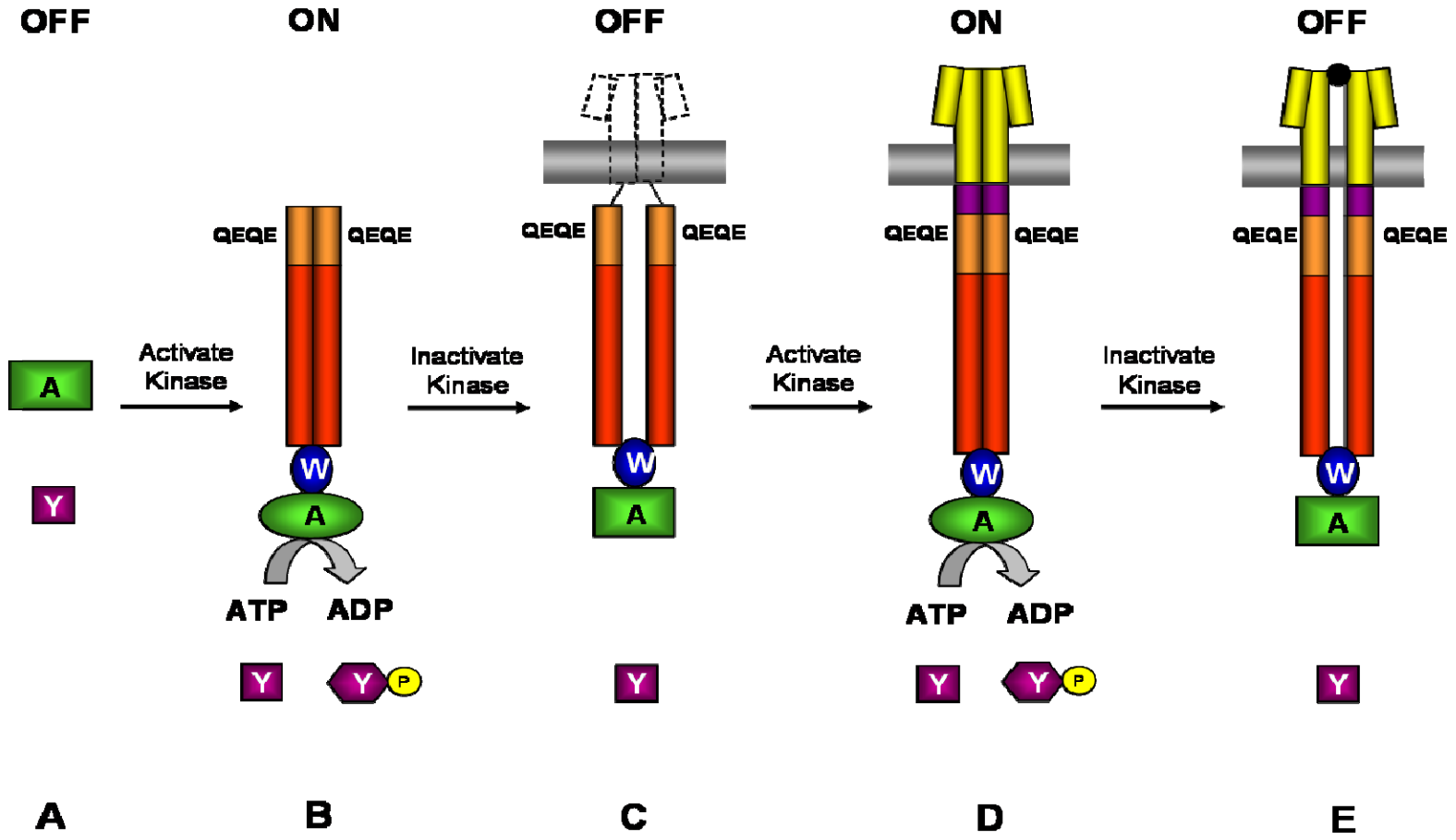

Fig. 9: Schematic illustration of the chemoreceptors influence on ChA kinase activity in the absence of adaptation machinery ($CheR^{-}B^{-}$). (A) In the absence of receptors, CheA kinase activity is very low, resulting in a low level of intracellular CheY-P. (B) When the cytoplasmic domain (red cylinder) is introduced into the system along with CheW, CheA is activated and phosphorylates CheY. (C) Addition of HAMP (purple cylinders) destabilizes the cytoplasmic domain four-helix bundle, inhibiting the kinase activating function of the cytoplasmic domain. (D) In the absence of attractant, kinase activity is restored when the periplasmic and transmembrane regions (yellow cylinders) are present, indicating that HAMP inhibition of the cytoplasmic domain is overcome. (E) The addition of attractant inhibits the HAMP-override imposed by the periplasmic/transmembrane region, allowing HAMP to once again inhibit stimulation of CheA.

REFERENCES

1. Adler, J. (1966) Chemotaxis in bacteria, *Science 153*, 708-716.

2. Tso, W. W., and Adler, J. (1974) Negative chemotaxis in *Escherichia coli*, *J Bacteriol 118*, 560-576.

3. Bibikov, S. I., Biran, R., Rudd, K. E., and Parkinson, J. S. (1997) A signal transducer for aerotaxis in *Escherichia coli*, *J Bacteriol 179*, 4075-4079.

4. Rebbapragada, A., Johnson, M. S., Harding, G. P., Zuccarelli, A. J., Fletcher, H. M., Zhulin, I. B., and Taylor, B. L. (1997) The Aer protein and the serine chemoreceptor Tsr independently sense intracellular energy levels and transduce oxygen, redox, and energy signals for Escherichia coli behavior, *Proc Natl Acad Sci U.S.A. 94*, 10541-10546.

5. Mesibov, R., and Adler, J. (1972) Chemotaxis toward amino acids in *Escherichia coli*, *J. Bacteriol 115*, 824-847.

6. Adler, J., Hazelbauer, G. L., and Dahl, M. M. (1973) Chemotaxis toward sugars in *Escherichia coli*, *J Bacteriol 115*, 824-847.

7. Manson, M. D., Blank, V., Brade, G., and Higgins, C. F. (1986) Peptide chemotaxis in *E. coli* involves the Tap signal transducer and the dipeptide permease, *Nature 321*, 253-256.

8. Khan, S., Pierce, D., and Vale, R. D. (2000) Interactions of the chemotaxis signal protein CheY with bacterial flagellar motors visualized by evanescent wave microscopy, *Current Biology 10*, 927-930.

9. Berg, H. C., and Anderson, R. A. (1973) Bacteria swim by rotating their flagellar filaments, *Nature 245*, 380-382.

10. Silverman, M., and Simon, M. (1974) Flagellar rotation and the mechanism of bacterial motility, *Nature 249*, 73-74.

11. Turner, L., Ryu, W. S., and Berg, H. C. (2000) Real-time imaging of fluorescent flagellar filaments, *J. Bacteriol. 182*, 2793-2801.

12. Macnab, R. M., and Koshland, D. E. (1972) The gradient-sensing mechanism in bacterial chemotaxis, *Proc Natl Acad Sci U.S.A. 69*, 2509-2512.

13. Berg, H. C., and Brown, D. A. (1972) Chemotaxis in *Escherichia coli* analysed by three-dimensional tracking, *Nature 239*, 500-504.

14. Brown, D. A., and Berg, H. C. (1974) Temporal stimulation of chemotaxis in *Escherichia coli*, *Proc Natl Acad Sci U.S.A. 71*, 1388-1392.

15. Segall, J. E., Block, S. M., and Berg, H. C. (1986) Temporal comparisons in bacterial chemotaxis, *Proc Natl Acad Sci U S A 83*, 8987-8991.

16. Krikos, A., Mutoh, N., Boyd, A., and Simon, M. I. (1983) Sensory transducers of *E. coli* are composed of discrete structural and functional domains, *Cell 33*, 615-622.

17. Kim, K. K., Yokota, H., and Kim, S. H. (1999) Four-helical-bundle structure of the cytoplasmic domain of a serine chemotaxis receptor, *Nature 400*, 787-792.

18. Ames, P., Yu, Y. A., and Parkinson, J. S. (1996) Methylation segments are not required for chemotactic signalling by cytoplasmic fragments of Tsr, the methyl-accepting serine chemoreceptor of *Escherichia coli*, *Mol Microbiol 19*, 737-746.

19. Liu, J. D., and Parkinson, J. S. (1991) Genetic evidence for interaction between the CheW and Tsr proteins during chemoreceptor signaling by *Escherichia coli*, *J Bacteriol 173*, 4941-4951.

20. Welch, M., Oosawa, K., Aizawa, S., and Eisenbach, M. (1993) Phosphorylation-dependent binding of a signal molecule to the flagellar switch of bacteria, *Proc Natl Acad Sci U.S.A. 90*, 8787-8791.

21. Roman, S. J., Meyers, M., Volz, K., and Matsumura, P. (1992) A chemotactic signaling surface on CheY defined by suppressors of flagellar switch mutations, *J. Bacteriol. 174*, 6247-6255.

22. Sourjik, V., and Berg, H. C. (2002) Binding of the Escherichia coli response regulator CheY to its target measured in vivo by fluorescence resonance energy transfer, *Proc Natl Acad Sci U S A 99*, 12669-12674.

23. Barak, R., and Eisenbach, M. (1992) Correlation between phosphorylation of the chemotaxis protein CheY and its activity at the flagellar motor, *Biochemistry 31*, 1821-1826.

24. Alon, U., Camarena, L., Surette, M. G., Aguera y Arcas, B., Liu, Y., Leibler, S., and Stock, J. B. (1998) Response regulator output in bacterial chemotaxis, *Embo J 17*, 4238-4248.

25. Hess, J. F., Oosawa, K., Matsumura, P., and Simon, M. I. (1987) Protein phosphorylation is involved in bacterial chemotaxis, *Proc. Natl. Acad. Sci. U. S. A. 84*, 7609-7613.

26. Segall, J. E., Manson, M. D., and Berg, H. C. (1982) Signal processing times in bacterial chemotaxis, *Nature 296*, 855-857.

27. Springer, M. S., Goy, M. F., and Adler, J. (1979) Protein methylation in behavioural control mechanisms and in signal transduction, *Nature 280*, 279-284.

28. Terwilliger, T. C., Bogonez, E., Wang, E. A., and Koshland, D. E., Jr. (1983) Sites of methyl esterification on the aspartate receptor involved in bacterial chemotaxis, *J. Biol. Chem. 258*, 9608-9611.

29. Terwilliger, T. C., and Koshland, D. E., Jr. (1984) Sites of methyl esterification and deamination on the aspartate receptor involved in chemotaxis, *J. Biol. Chem. 259*, 7719-7725.

30. Kehry, M. R., Bond, M. W., Hunkapiller, M.W., and Dahlquist, F.W. (1983) Enzymatic deamidation of methyl-accepting chemotaxis proteins in *Escherichia coli* catalyzed by the *cheB* gene product, *Proc Natl Acad Sci U.S.A. 80*, 3599-3603.

31. Goy, M. F., Springer, M. S., and Adler, J. (1977) Sensory transduction in *Escherichia coli*: role of a protein methylation reaction in sensory adaptation, *Proc Natl Acad Sci U.S.A. 74*, 4964-4968.

32. Silverman, M., and Simon, M. (1977) Chemotaxis in Escherichia coli: methylation of che gene products, *Proc Natl Acad Sci U.S.A. 74*, 3317-3321.

33. Kondoh, H., C.B. Ball, and J. Adler. (1979) Identification of a methyl-accepting chemotaxis protein for the ribose and galactose chemoreceptors of *Escherichia coli*, *Proc Natl Acad Sci U.S.A. 76*, 260-264.

34. Hazelbauer, G. L. a. E., P. (1980) Parallel pathways for transduction of chemotactic signals in *Escherichia coli*, *Nature 283*, 98-100.

35. Bibikov, S. I., Miller, A.C., Gosink, K.K, and Parkinson, J.S. (2004) Methylation-independent aerotaxis mediated by the *Escherichia coli* Aer protein, *J. Bacteriol 186*, 3730-3737.

36. Ames, P., Studdert, C. A., Reiser, R. H., and Parkinson, J. S. (2002) Collaborative signaling by mixed chemoreceptor teams in *Escherichia coli*, *Proc Natl Acad Sci U.S.A. 99*, 7060-7065.

37. Studdert, C. A., and Parkinson, J. S. (2005) Insights into the organization and dynamics of bacterial chemoreceptor clusters through *in vivo* crosslinking studies, *Proc Natl Acad Sci U.S.A. 102*, 15623-15628.

38. Studdert, C. A., and Parkinson, J. S. (2004) Crosslinking snapshots of bacterial chemoreceptor squads, *Proc Natl Acad Sci U.S.A. 101*, 2117-2122.

39. Ames, P., and Parkinson, J. S. (2006) Conformational suppression of inter-receptor signaling defects, *Proc Natl Acad Sci U.S.A. 103*, 9292-9297.

40. Milligan, D. L., and Koshland, D. E., Jr. (1988) Site-directed cross-linking. Establishing the dimeric structure of the aspartate receptor of bacterial chemotaxis, *J Biol Chem 263*, 6268-6275.

41. Bowie, J. U., Pakula, A. A., and Simon, M. I. (1995) The three-dimensional structure of the aspartate receptor from *Escherichia coli*, *Acta Crystallogr D Biol Crystallogr 51*, 145-154.

42. Milburn, M. V., Prive, G. G., Milligan, D. L., Scott, W. G., Yeh, J., Jancarik, J., Koshland, D. E., Jr., and Kim, S. H. (1991) Three-dimensional structures of the ligand-binding domain of the bacterial aspartate receptor with and without a ligand, *Science 254*, 1342-1347.

43. Scott, W. G., Milligan, D. L., Milburn, M. V., Prive, G. G., Yeh, J., Koshland, D. E., Jr., and Kim, S. H. (1993) Refined structures of the ligand-binding domain of the aspartate receptor from *Salmonella typhimurium*, *J Mol Biol 232*, 555-573.

44. Draheim, R. R., Bormans, A. F., Lai, R. Z., and Manson, M. D. (2006) Tuning a bacterial chemoreceptor with protein-membrane interactions, *Biochemistry 45*, 14655-14664.

45. Ottemann, K. M., Xiao, W., Shin, Y. K., and Koshland, D. E., Jr. (1999) A piston model for transmembrane signaling of the aspartate receptor, *Science 285*, 1751-1754.

46. Draheim, R. R., Bormans, A. F., Lai, R. Z., and Manson, M. D. (2005) Tryptophan residues flanking the second transmembrane helix (TM2) set the signaling state of the Tar chemoreceptor, *Biochemistry 44*, 1268-1277.

47. Aravind, L., and Ponting, C. P. (1999) The cytoplasmic helical linker domain of receptor histidine kinase and methyl-accepting proteins is common to many prokaryotic signalling proteins, *FEMS Microbiol Lett 176*, 111-116.

48. Williams, S. B., and Stewart, V. (1999) Functional similarities among two-component sensors and methyl-accepting chemotaxis proteins suggest a role for linker region amphipathic helices in transmembrane signal transduction, *Mol Microbiol 33*, 1093-1102.

49. Bass, R. B., and Falke, J. J. (1998) Detection of a conserved alpha-helix in the kinase-docking region of the aspartate receptor by cysteine and disulfide scanning, *J Biol Chem 273*, 25006-25014.

50. Bass, R. B., Coleman, M. D., and Falke, J. J. (1999) Signaling domain of the aspartate receptor is a helical hairpin with a localized kinase docking surface: cysteine and disulfide scanning studies, *Biochemistry 38*, 9317-9327.

51. Bass, R. B., and Falke, J. J. (1999) The aspartate receptor cytoplasmic domain: *in situ* chemical analysis of structure, mechanism and dynamics, *Structure 7*, 829-840.

52. Hulko, M., Berndt, F., Gruber, M., Linder, J. U., Truffault, V., Schultz, A., Martin, J., Schultz, J. E., Lupas, A. N., and Coles, M. (2006) The HAMP domain structure implies helix rotation in transmembrane signaling, *Cell 126*, 929-940.

53. Swain, K. E., and Falke, J. J. (2007) Structure of the conserved HAMP domain in an intact, membrane-bound chemoreceptor: a disulfide mapping study, *Biochemistry 46*, 13684-13695.

CONTACT INFORMATION

Name:	Rachel Leann Crowder
Professional Address:	c/o Dr. Michael Manson Department of Biology MS 3258 Texas A&M University College Station, TX 77843
Email Address:	rcrowder@tamu.edu
Education:	B.S., Biology, Texas A&M University, May 2009 Undergraduate Research Scholar NSF LSAMP Undergraduate Research Scholar Honors Program Lechner Scholarship Recipient